Optically trapped microsensors for microfluidic temperature measurement by fluorescence lifetime imaging microscopy

Post-print of a peer-reviewed article published by the Royal Society of Chemistry.
Published article available at: http://dx.doi.org/10.1039/C1LC20391F

Cite as:
Bennet, M. A., Richardson, P. R., Arlt, J., McCarthy, A., Buller, G. S., & Jones, A. C. (2011). Optically trapped microsensors for microfluidic temperature measurement by fluorescence lifetime imaging microscopy. *Lab on a Chip*, 11(22), 3821-3828.

Manuscript received: 06/05/2011; Accepted: 31/08/2011; Article published: 28/09/2011

Optically trapped microsensors for microfluidic temperature measurement by fluorescence lifetime imaging microscopy**

Mathieu A. Bennet,[1,2] Patricia R. Richardson,[1,2] Jochen Arlt,[2,3] Aongus McCarthy,[4] Gerald S. Buller[4] and Anita C. Jones[1,2,*]

[1]EaStCHEM, School of Chemistry, Joseph Black Building, University of Edinburgh, West Mains Road, Edinburgh, EH9 3JJ, UK.

[2]Collaborative Optical Spectroscopy, Micromanipulation and Imaging Centre (COSMIC), King's Buildings, The University of Edinburgh, EH9 3JZ, UK.

[3]SUPA, School of Physics, King's Buildings, University of Edinburgh, EH9 3JZ, UK.

[4]School of Engineering and Physical Sciences, Heriot-Watt University, Edinburgh, EH14 4AS, UK.

[*]Corresponding author; e-mail: a.c.jones@ed.ac.uk, fax: +44 (0) 1316504753

[**]We are grateful to the Engineering and Physical Sciences Research Council (GR/S96555/01) and the National Physical Laboratory (sponsorship of MAB's studentship) for funding. We thank Dr David Mendels for helpful discussions, Dr Nhan Pham for assistance with the development of the microfluidic device, and Mr Andrew Garrie for technical support.

Supporting information:
Electronic supplementary information (ESI) available. See http://dx.doi.org/10.1039/C1LC20391F

Graphical abstract:

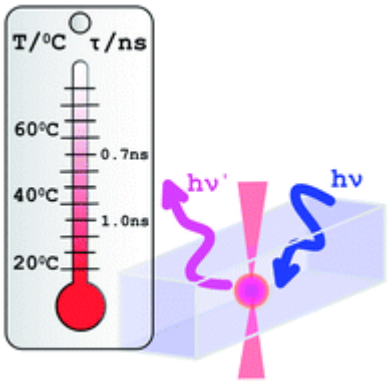

Abstract

The novel combination of optical tweezers and fluorescence lifetime imaging microscopy (FLIM) has been used, in conjunction with specially developed temperature-sensitive fluorescent microprobes, for the non-invasive measurement of temperature in a microfluidic device. This approach retains the capability of FLIM to deliver quantitative mapping of microfluidic temperature without the disadvantageous need to introduce a fluorescent dye that pervades the entire micofluidic system. This is achieved by encapsulating the temperature-sensitive Rhodamine B fluorophore within a microdroplet which can be held and manipulated in the microfluidic flow using optical tweezers. The microdroplet is a double bubble in which an aqueous droplet of the fluorescent dye is surrounded by an oil shell which serves both to contain the fluorophore and to provide the refractive index differential required for optical trapping of the droplet in an external aqueous medium.

Introduction

With the emergence of ever new applications in microfluidic technology, innovative methods to measure environmental and chemical properties within microchannels are required. Precise control of temperature is a key requirement in many microfluidic applications, for example, in biology for polymerase chain reaction amplification of DNA,[1, 2] in medicine for drug delivery,[3] in electronics for heat dissipation[4] and in chemistry for control of reaction rates, determination of phase transition temperatures and activation energies.[5] However, the measurement of temperature on such a small scale is challenging. To date, attempts to measure temperature within microfluidic devices have been based on a number of different mechanical and optical approaches.

Conventionally, temperature in microfluidics is measured via micro-thermocouples integrated within each chip. However, a major drawback to this approach is that it can only report the temperature of a very small volume of solution close to the thermocouple itself. It is well known that rapid heat dissipation within microfluidic devices can lead to significant non-uniformity of the temperature over the small intra-channel length scales, and, thus, micro-thermocouples can, at best, only provide an approximate spatial temperature map. Additionally, the necessity of implanting the thermocouple within the device reduces measurement flexibility, and requires complex fabrication routes coupled with shortened device lifespan.

As an alternative, optical techniques are currently being developed to overcome some of the limitations of micro-thermocouples. Common approaches utilise the temperature sensitivity of the commercially available fluorescent dye Rhodamine B (RhB) combined with fluorescence intensity techniques.[6-11] However, such approaches are also beset with problems, for example, the adsorption of RhB on the internal surfaces of the device, which affects intensity and lifetime, photobleaching of the fluorescent

probe[11] and variations in the excitation and detection efficiencies across the field of view of the microscope can all result in artefacts in the measurement.[12] The use of methods based on the measurement of the fluorescence lifetime of a dye, such as fluorescence lifetime imaging microscopy (FLIM), overcomes some of these problems, and FLIM has been used successfully to generate high spatial resolution maps of temperature distribution in microfluidic devices.[13-16] Use of a customised polymer based temperature-sensitive fluorescent probe allowed the temperature in a microfluidic device to be measured with a resolution of less than 0.1ºC.[17] While FLIM offers high spatial resolution and accurate mapping of the temperature in devices, the technique also exhibits some drawbacks since the fluorescent dye pervades the whole measurement volume. Although this may not be problematic for measurements on prototype devices during design and development, it precludes application in functioning microfluidic systems where the presence of the dye would interfere with the function. Such applications include microreactors, where the presence of the dye could interfere with chemical reactions, and biological application involving permeable cells, where toxicity of the dye molecules can be problematic. Cells can be damaged or killed by direct chemical toxicity of the dye and also through dye-induced photosensitisation.[18] Attempts to overcome the problem of dye toxicity, by incorporating RhB into the polymer of the device,[11] suffered the same shortcomings as both microthermocouples and fluorescence intensity-based methods, namely local artefacts and inaccurate measurement of the temperature in the channel.

The Brownian motion of nanoparticles has been proposed as an alternative technique to perform three dimensional measurement in microsystems and avoid toxicity effects.[12] While the nanoparticles used were not toxic to the system studied in the published work, using Brownian motion is only feasible when there is no fluid motion. The requirement to measure the temperature while the device is in operation without introducing perturbations is, therefore, only fulfilled in the case of stop flow operation with biological objects not sensitive to the nanoparticles tracked.

To date, techniques that have been used to measure temperature in microfluidic devices all have drawbacks. To address these drawbacks we have developed an alternative method which permits the use of FLIM without the disadvantageous use of an intrusive fluorescent dye. This has been achieved by encapsulating the temperature sensitive RhB fluorophore within a chemically inert microdroplet, which can be held and manipulated in the flow using optical tweezers.

Optical tweezers have been used previously to manipulate objects within microfluidic devices, for example, to analyse flow fields by measuring the displacement of trapped beads,[19-21] as micropumps or microvalves,[22-24] for cell manipulation alone[25] or associated with a visualisation technique such as fluorescence microscopy,[26] super resolution microscopy[27] or Raman spectroscopy.[28] Gullapalli *et al*[29] report the implementation of time-resolved fluorescence and an optical trap on the same microscope, but do not appear to have used them simultaneously to record the fluorescence lifetime of a trapped object. A fluorescein-labelled polymer bead has been trapped in a microfluidic device and its fluorescence intensity measured to determine the local pH.[30]

In principle, a similar approach using a RhB-labelled bead might be used to measure temperature. However, we have found that immobilisation of RhB on a polymer bead inhibits the intramolecular torsional motion that is the origin of the temperature sensitivity of the fluorophore.[31] We investigated commercially available RhB-loaded polystyrene beads and custom-synthesised surface-functionalised beads in which the fluorophore is tethered to the surface by an alkyl amino chain.[32] For both types of bead the RhB lifetime was independent of temperature. To overcome this problem, we have used a water-oil-water emulsification method[33] to produce microdroplets in which the RhB fluorophore is encapsulated but remains in a fluid environment. In these 'double bubbles' an aqueous droplet of the fluorescent dye, Kiton Red (a water-soluble, sulfonated derivative of RhB), is surrounded by an oil shell which serves both to contain the fluorophore and to provide the refractive index differential required for optical trapping of the droplet in an external aqueous medium.

Our novel method combines the capability of optical tweezers to manipulate objects with the capacity of FLIM to provide quantitative temperature measurement. It allows the temperature to be measured locally, with micron-scale spatial resolution while the microsystem is in operation without introducing artefacts or toxicity to the continuous flowing medium.

Materials and Methods

Microfluidic Device & Generation of Temperature Gradient

The microfluidic devices were fabricated using soft lithography.[34] The mould was fabricated by UV photolithography using a negative photoresist (SU8-2025, Microchem, Newton, MA) and developed in a SU8 developer (propylene glycol monomethyl ether acetate, Microchem). The mould was then treated with fluorosilane (1H,1H,2H,2H-perfluorodecylthriethoxysilane, Sigma-Aldrich) to prevent adhesion of the PDMS (Sylgard 184, Dow Corning Midland, MI). A PDMS mixture of 10:1 polymer to hardener ratio was degassed, poured onto the wafer and cured for 2 hours at 70ºC. Inlets and outlets were punched with cutting tips (Uni-core, Harris Redding CA). After oxygen plasma treatment (50W, 30s, 0.300 Torr) the device was sealed by fusion with a microscope coverslip (L4239-1, Agar Scientific Ltd, England).

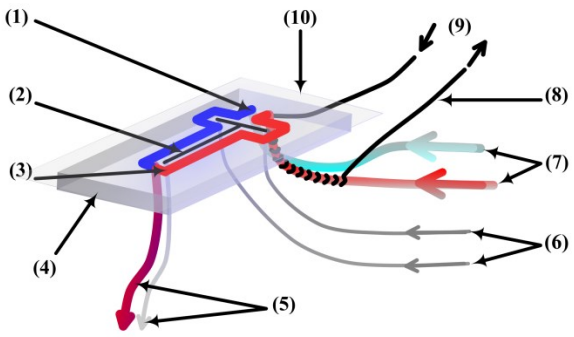

← ***Figure 1.*** Schematic representation of the microfluidic device: cooling channel (1); microchannel (2); heating channel (3); PDMS substrate (4); outlets (5); tubing delivering sample to microfluidic channel inlets (6); tubing delivering hot (red) and cold (blue) fluid to heating/cooling channel inlets (7); nichrome wire (8) and heating current (9); optical window (microscope coverslip) (10).

As illustrated in Figure 1, the microfluidic device comprises two independent channel networks: the microchannel (200 μm wide and 100 μm deep) and, separated by a PDMS wall (100 μm wide), the channels controlling the temperature (400 μm wide and 100 μm deep). The diluted micro-emulsion (ca 50μl of the micro-emulsion in 10ml of the water phase (W2)) was pumped into the microchannel using syringe pumps (KDScientific, Holliston, MA; 1ml Syringe, BD, Belgium) through PEEK tubing (Tub PEEK™ Yel, Upchurch Scientific, Oak Harbor, WA (BD) at a flow rate of 0.05μl/min. The channels that control the temperature are separated from the microchannel by a PDMS wall 100μm thick. Hot/cold water is pumped into the heating/cooling channel by a syringe pump. Water was heated by a Nichrome wire coil around the inlet tubing, the temperature of the heating coil was controlled by varying the current (ca. 500mA) supplied by a DC power supply (Thurlby Thandar TS3022S). Typical flow rate was 350μl/min for the heating/cooling channels.

Optical Tweezers

The combination of FLIM and optical tweezers was implemented on a custom-built multi-parameter microscope platform, specifically designed to enable the simultaneous application of multiple imaging modalities. The microscope platform was constructed from a 650 mm × 400 mm × 25 mm thick baseplate of aluminium which had a designed network of fixed-width slots machined into its surface. The slots act as convenient and flexible, semi-kinematic alignment channels for custom-designed optomechanical component mounts. The optomechanical mounts are held in place in the slots with small magnets. The baseplate is mounted above the optical bench in an upright microscope configuration. A sub-micron resolution xyz translation stage located underneath the objective carousel is used to position the sample. The design and construction of this microscope will be described in detail elsewhere. The optical arrangement is shown schematically in Figure 2.

The custom-built optical tweezers system[35] allows trapping and manipulation of micron-sized particles using an intuitive ‘click and trap’ computer interface. The circularised, diffraction-limited output beam from a laser diode package with an output power of up to 70 mW at a wavelength of 785 nm (VPSL-0785-070-X-5-A, Blue Sky Research), was used to form the optical trap. The laser beam is expanded and then coupled into the back of the microscope objective (60x, NA 1.2 Plan Apo WI, Nikon), using a 780-nm short-pass dichroic mirror. The high numerical aperture of the water immersion objective ensured a tight focussing of the beam and resulted in strong trapping while at the same time minimising aberrations when trapping deep inside the sample. The laser beam can be steered using a pair of galvanometric mirrors located in the conjugate plane of the objective’s back aperture. The graphical user interface (written in Labview 7.1, National Instruments) displays live images of the sample captured on a CCD camera and adjusts the trap position by controlling the galvanometric mirrors in response to mouse movement.

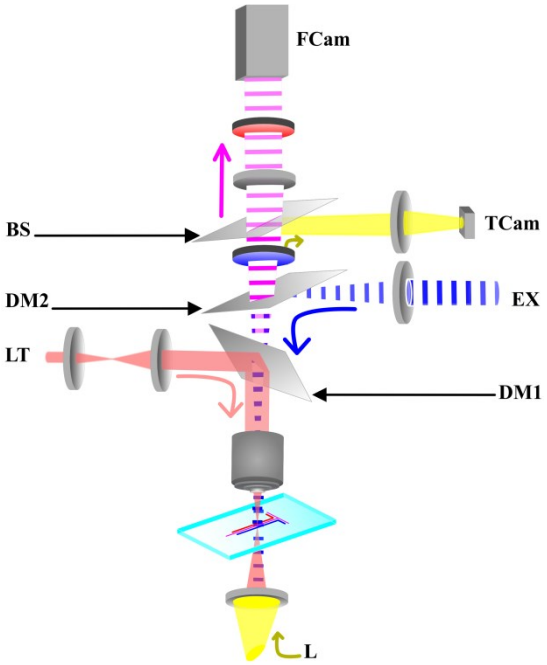

Figure 2. Schematic diagram of the optical setup in which optical trapping and fluorescence lifetime imaging microscopy are combined. L: white illumination light; LT: laser tweezers beam (red line); DM1: dichroic mirror 1 (transmission below 780nm); DM2: dichroic mirror 2 (transmission above 505nm); EX: excitation source (blue dashed line); BS:beam splitter; TCam: tweezer control camera; FMCam: FLIM camera; fluorescence signal (pink dashed line).

Fluorescence lifetime imaging microscopy

A 468-nm diode laser (LDH-P-C-470, Picoquant GmbH, Germany) controlled by a picosecond pulsed driver (PDL800-B, Picoquant GmbH), pulse width <90 ps FWHM, operating at 40 MHz was used as the excitation source for FLIM. The beam was reshaped using a pair of semi-cylindrical lenses, expanded and collimated, spatially filtered through an aperture and focused at the back focal plane of the microscope objective following reflection off a dichroic mirror. The fluorescence was collected through the same objective. Unwanted scattered light from the excitation source and the laser tweezers was removed using bandpass filters The fluorescence was imaged onto a gated intensified CCD camera (Picostar HR-12QE, LaVision GmgH, Germany) using an achromatic doublet lens. FLIM images were recorded with 1ns gate widths at 1 ns intervals, in accordance with established practice.[36] Five images were averaged to create the final image. The exposure time of the camera was set (in the range 340 ms to 680 ms) to obtain a maximum intensity per pixel of between 3000 and 4000 counts. The instrument response function was recorded by using a mirror in place of the sample. It was thus established that the fluorescence decay could be fitted from 1 ns after the emission peak image without distortion by the instrument response.

FLIM images were produced and analysed using DaVis 6.2 software, as described previously.[17]

Preparation and characterisation of fluorescent microdroplets

The fluorescent microdroplets consisted of an aqueous solution of the fluorescent dye encapsulated inside an oil bubble, which in turn was suspended in an external water phase. Similar water-oil-water emulsions have been used for *in-vitro* compartmentalisation,[33, 37-39] and the protocol used here for emulsion preparation was adopted from this previous work. The internal water phase (W1) was an aqueous solution of 0.3 mM Kiton Red (Sulforhodamine B, acid form, laser grade, Sigma-Aldrich) and 0.3 mM NaCl. The oil phase (O) consisted of paraffin oil (Fisher Scientific) and a surfactant 3.2% wt/wt (ABIL EM 90, Degussa). The external water phase (W2) was an aqueous solution of 1% wt/wt of a surfactant (Triton X-102, Sigma-Aldrich) and 0.75% of carboxymethyl cellulose (Sigma-Aldrich). Each phase was homogenised separately in a sonic bath at room temperature and shaken regularly for 1 hour, then cooled over ice. Over ice, 25 µl of W1 was added to 2 ml of O and homogenised (Disperser, Ultra-Turrax T25 basic, Ika®) for 2 min at 13500 rpm, to create a water in oil (W1/O) emulsion. Over ice, 2.4 ml of W2 was added to the emulsion W1/O, and homogenised for 2 min at 11500 rpm, to form the final W1/O/W2 emulsion. A dilute solution of microdroplets was then produced by dilution of 50µl of the W1/O/W2 emulsion into 10ml of W2.

Water-in-oil microemulsions of the type used here were developed originally for *in vitro* compartmentalisation of genetic, biochemical and cell-based assays,[33,37-39] with each droplet acting as a microreactor. The surfactant present in the oil phase of the micropdroplets is, therefore, compatible with such assays. In the present work, for convenience, the concentrated emulsion was diluted into the same surfactant-containing aqueous phase as used in the initial emulsification, to give a sample of microdroplets that was stable over many days. For applications in which the presence of a surfactant, such as 1% Triton X-102, in the outer aqueous phase could be problematic, such as cell-based assays, the concentrated microemulsion could be diluted into aqueous buffer (surfactant-free), as described in previously published protocols,[33] thus reducing the concentration of surfactant to a level well below that which would be harmful to cells.[40]

The temperature response of the fluorescence lifetime of the emulsion was measured by time-correlated single photon counting in an Edinburgh Instruments spectrometer equipped with TCC900 photon counting electronics, as described previously.[17] A sample of the emulsion in a 1-cm path-length microcuvette (500 µl sample volume) held in a thermostatically controlled cuvette holder. The temperature was measured with a thermocouple (Hanna Instruments HI93530) immersed directly in the emulsion. Fluorescence was excited at 400nm and detected at 580nm, via a 488-nm long-pass filter (Semrock) and a monochromator which was set to a band-pass of 18 nm to mimic the band-pass filter used in the FLIM setup. Decay curves were recorded over a time range of 50 ns, resolved into 4096 channels and accumulated to give 10000 counts in the peak channel. The instrument response of the system, measured using an aqueous suspension of Ludox scatterer, was approximately 90 ps FWHM. The time-resolved data were fitted to a multiexponential decay function (Eq. 1), using FAST software (Edinburgh Instruments).

$$I(t) = \sum_{i=1}^{n} A_i \exp\left(\frac{-t}{\tau_i}\right) + B \qquad (1)$$

where τ_i is the fluorescence lifetime, A_i (the "A-factor") is the fractional amplitude of the i^{th} decay component, and B is the background (dark count of the detector). In the present case, where the different lifetime components correspond to the same fluorophore in different environments (and may be assumed to have the same radiative lifetime), the A-factor indicates the fraction of the emitting molecules that has a particular lifetime, τ_i. The quality of the fits was determined by the value of the reduced chi-squared statistical parameter and by visual inspection of residuals.

Results and discussion

The response of microdroplet fluorescence lifetime to temperature

The fluorescence decay of a dilute solution of KR microdroplets (50µl of initial formulation into 10ml of W2) was measured as a function of temperature over the range 27 ºC to 61 ºC. At each temperature, the fluorescence decay was described by a bi-exponential function. The decay parameters together with the average lifetimes, $\langle\tau\rangle$, as defined by Eq. 2, are given in Table 1.

$$\langle\tau\rangle = \frac{A_1\tau_1 + A_2\tau_2}{A_1 + A_2} \qquad (2)$$

Table 1. Temperature-dependence of the fluorescence decay parameters of Kiton Red microdroplets. The fluorescence lifetimes, τ_i, and the corresponding fractional amplitudes, A_i, are given, together with the average lifetime, $\langle\tau\rangle$.

Temp. / ºC	T_1 / ns	$\tau_{2\,/}$ ns	A_1	A_2	$\langle\tau\rangle$ / ns
27.0	1.23	2.32	0.80	0.20	1.45
35.2	1.04	2.17	0.87	0.13	1.19
44.0	0.86	2.29	0.93	0.07	0.96
52.7	0.69	2.53	0.96	0.04	0.77
61.4	0.57	3.17	0.97	0.03	0.64

The predominant shorter lifetime component, τ_1, accounts for 80% of the emitting population at 27 ºC, increasing to 97% at 61.4 ºC. The value of τ_1 corresponds to that of KR in bulk aqueous solution[13], where the decay is mono-exponential. The second, minor component with longer lifetime, τ_2, suggests the presence of dye aggregates in the microdroplet. The less soluble parent fluorophore, Rhodamine B, readily forms aggregates in water even at micro-molar concentrations, characterised by the appearance of a longer lifetime component in the fluorescence decay.[41] It is, therefore, not surprising to observe a small amount of

aggregation of KR at a concentration of 0.3 mM. Furthermore, the decrease of the amplitude of this component (A_2) with increasing temperature is consistent with disaggregation at higher temperature, as observed previously.[42]

The bi-exponential decay of the microdroplets can be conveniently represented by a single parameter, the average lifetime $<\tau>$, as defined by Eq. 2. The values of $<\tau>$ are given in Table 1. The dependence of $<\tau>$ on temperature is shown graphically in Figure 3, together with the corresponding curve for KR in bulk water.

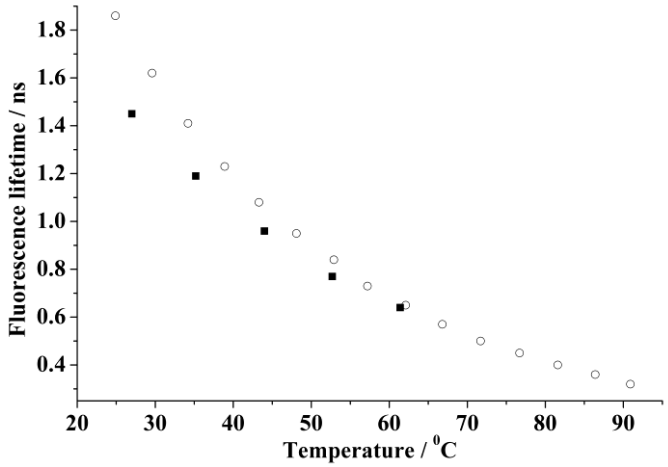

Figure 3. Temperature dependence of the average fluorescence lifetime of Kiton Red microdroplets (■). The corresponding temperature dependence in bulk aqueous solution (○),[13] is shown for comparison.

The lifetime-temperature response of the microdroplets resembles that of the bulk solution,[13] confirming that containment of KR in the microdroplet does not inhibit its conformational freedom. The small decrease in lifetime of KR in the microdroplets compared with bulk aqueous solution may be accounted for by the effect of the local environment (presence of NaCl and surfactants and the proximity of an oil/water interface) on the non-radiative decay rate and the effect of increased refractive index, which increases the radiative rate.[43]

Construction of the calibration curve to be applied to FLIM measurements

In order to construct a calibration curve of temperature versus lifetime to apply to the FLIM data it is necessary to fit the decays acquired by TCSPC over the same time range as that used when fitting the data recorded using the FLIM system, from 1ns after the decay peak to 8ns after the decay peak. Over this truncated range, the decays could be fitted satisfactorily by single exponential functions. This is demonstrated in Table 2, where the decay times obtained from single exponential fitting can be seen to be in very good

agreement with the average lifetimes derived from bi-exponential fitting over the same range. Thus the FLIM data can be analysed by single exponential fitting and the derived lifetimes converted to temperature using the calibration curve shown in Figure 4. The relationship between temperature and lifetime can be represented by an exponential function, as demonstrated previously for KR in bulk aqueous solution.[13]

Table 2. Fluorescence lifetimes obtained from fitting the TCSPC data over the truncated time range that corresponds to the FLIM decay data. The fluorescence lifetimes obtained from single exponential fitting function, τ_s, are compared with the average lifetimes, $<\tau>$, derived from bi-exponential fitting.

Temp. / ^oC	τ_s /ns	$<\tau>$ /ns
27.0	1.51	1.54
35.2	1.26	1.27
44.0	1.06	1.10
52.7	0.90	0.91
61.4	0.79	0.84

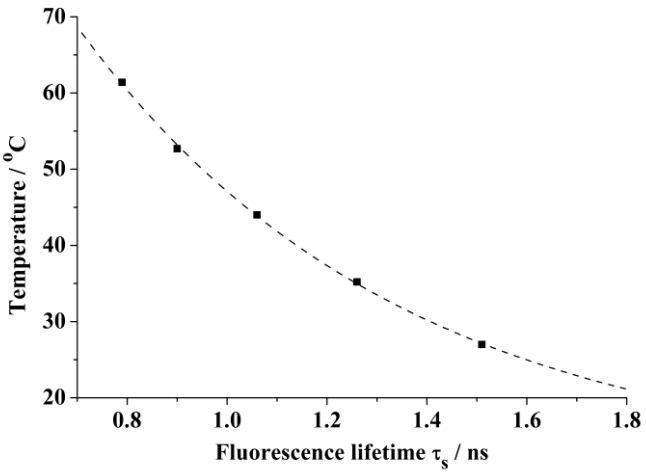

Figure 4. Calibration curve relating temperature to the fluorescence lifetime of the microdroplet, the dashed line shows the exponential function fitted to the data
($T = 172.086\exp(-\tau/0.645)+10.515$) that was used for subsequent analysis of the FLIM images.

Fluorescence lifetime imaging microscopy of optically trapped microdroplets in the microchannel

The use of optical tweezers necessitates high magnification and large numerical apertures to produce a very tightly focused beam, in combination with moderate optical powers, in order to enable the capture of an object subject to Brownian motion and flow. This naturally raises concerns about heating effects, which may perturb device operation or damage biological samples. Previous work has shown that heating due to the tweezer beam is wavelength-dependent and scales linearly with power.[44-47] The temperature increase due to a

comparable 800-nm tweezer was reported to be 1.7ºC/W.[47] The 780-nm laser tweezer, used in the present experiments, has a maximum output power of 60mW, which, assuming no loss along the optical path, would induce a temperature increase of 0.1ºC. This small temperature increase should not perturb the device operation, would not damage biological samples and does not introduce any artefact into the temperature measurement since 0.1ºC is below the temperature resolution of KR FLIM (*vide infra*). The absence of a discernible heating effect was confirmed by FLIM of microdroplets in the absence and presence of the tweezer laser beam.

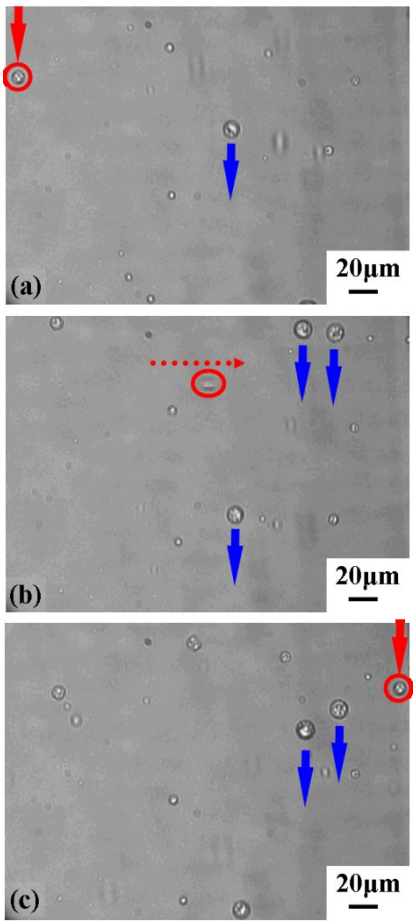

Figure 5. A series of frames from the tweezer-control camera showing the trapping and manoeuvring of a microdroplet. The optical power was 40 mW and the flow rate was 0.1 µl min^{-1}. (a) The position at which the microdroplet was initially trapped (red arrowhead) at the left-hand edge of the channel. (b) Movement of the microdroplet to the centre of the channel (red dotted arrow). (c) The microdroplet in its final position at the right-hand edge of the channel. For spatial reference the position and motion of some untrapped microdroplets are indicated by blue arrowheads. A video of optical trapping is available as Supporting Information.

Microdroplets could be trapped at powers just above the lasing threshold (ca. 3 mW) in the absence of flow, whilst at maximum output optical power droplets could be trapped in a flow velocity of up to 1mm/s (2 μl/min). Once trapped, a microdroplet was moved to the desired position and a series of time-gated images recorded in order to generate a FLIM image. Figure 5 shows a series of frames from the tweezer-control camera illustrating the capture and positioning of a droplet in the microchannel. A video can be seen in the Supplemenatry Information.

Figure 6(a) and (b) show the intensity image of a microdroplet trapped in the flow together with the corresponding intensity profile. In order to generate the FLIM image, pixels with low intensity were rejected by setting a threshold equal to the half-maximum of the intensity profile. The FLIM map of the droplet generated is shown in Figure 6 (c). The fluorescence decay, constructed by integrating the intensity at each gate over the entire droplet image, is shown in Figure 6(d). As anticipated, the FLIM decays were well fitted by single exponential functions.

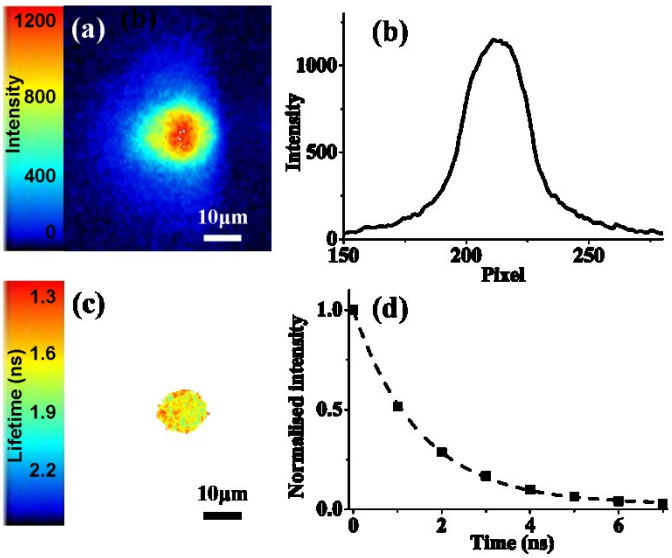

Figure 6. (a) Fluorescence intensity image of a microdroplet trapped in the microfluidic channel. (b) Intensity profile across the droplet. (c) FLIM image of the droplet. (d) Fluorescence decay data (black dots) extracted from the FLIM image of the entire droplet and the fitted single exponential function (dotted curve). The lifetime is 1.52 ns corresponding to a temperature of 26.9 ^{o}C.

Figure 7 shows the FLIM images of a droplet trapped at three different positions (see Figure 5) in the temperature gradient across the microfluidic channel. These images clearly show the change of fluorescence lifetime of the droplet associated with the change of local temperature. The average fluorescence lifetime of

the droplet changes from 1.37±0.04ns in 7(a) to 1.52±0.03 ns in 7(b) to 1.80±0.07ns in 7(c), corresponding to temperatures of 31.1±1.3 ºC, 26.9±0.8 ºC and 21.1±1.1 ºC, respectively.

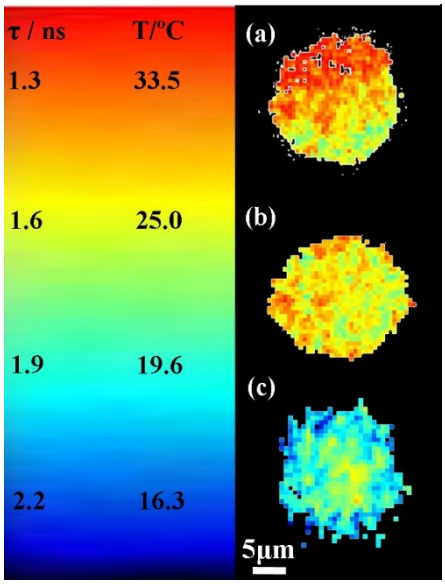

Figure 7. FLIM images of a droplet trapped at three different positions in the temperature gradient across the microfluidic channel: (a) high temperature; (b) intermediate temperature; (c) low temperature. The colour coded scale illustrates the fluorescence lifetime calculated at each pixel.

The spatial distribution of the fluorescence lifetimes in the image in Figure 7(a) is noticeably non-uniform, compared with the other two FLIM images; there appears to be a gradient of fluorescence lifetime values across the microdroplet. We believe that this is an artefact due to a slight movement of the microdroplet during the time-gated image acquisition (*ca*. 1 minute). For regions of the droplet where there is a significant intensity gradient in the direction of motion, movement of the droplet will contribute to the change in pixel intensity between time gates. In the present work, data from the shortest delay times were acquired first. Thus, if the motion results in a significant decrease in pixel intensity with time during data acquisition, the apparent fluorescence decay time for that pixel will be shortened, and vice versa. From the apparent lifetime gradient across the droplet in Figure 7(a) we would infer that the droplet has moved downwards during the acquisition and this indeed corresponds to the direction of fluid flow in the channel. The size of the optical trap is much smaller than the microdroplet and it is possible that the microdroplet has moved due to forces exerted by the flow while remaining in the trap. The degradation of time-gated FLIM images by motion artefacts has been observed previously by Elson et al.[48] who showed that the movement of fluorescent beads (not optically trapped) resulted in a change in the intensity of some areas of the beads between time-gated images with a consequent change in apparent fluorescence lifetime in these areas. This motion artefact could be problematic

if the spatial distribution of the fluorescence lifetimes were being used to quantify local environmental characteristics. However, in the present case, the lifetime value used to determine the temperature is calculated from intensity data integrated over the entire droplet, and, therefore, is unaffected by droplet motion.

In principle, the spatial resolution of temperature measurement that could be obtained with microdroplet probes is limited by the size of the microdroplets themselves. Their diameter is adjustable by varying the emulsification procedure used during their preparation. Stable microdroplets can be produced down to diameters around 70 nm.[33]. However, in the present study, a minimum droplet diameter of about 5 μm was necessary to obtain sufficient fluorescence intensity for detection. The use of a more sensitive, photon counting detector and a more favourable excitation wavelength (our 468-nm diode laser is far from optimum; the absorption maximum of KR is at 565 nm) would allow smaller droplets to be detected. Using the present optical tweezers system, droplets down to ~ 1 μm in diameter could be trapped. Trapping particles much smaller than the wavelength of light is challenging. However, optical trapping of 50-100 nm particles has been demonstrated.[49] There is also scope for greater temperature resolution by encapsulating a more sensitive fluorescent probe within the microdroplet, for example the recently reported thermo-responsive polymer would permit a temperature resolution of less than 0.1 ºC.[17] The implementation of multiple-trap optical tweezers would enable multiplex measurements at different positions within the microfluidic device or the simultaneous use of different microprobes, for example KR for low resolution over a large temperature range and various thermo-responsive polymers for high resolution over small temperature ranges.

Conclusion

The ability to combine optical tweezers and FLIM, facilitated by the use of a custom-built multi-modal microscope, has permitted us to develop a new, non-invasive approach to microfluidic temperature measurement, based on the well known temperature-dependence of the Rhodamine B fluorophore.

Temperature-sensitive fluorescence lifetime microprobes have been fabricated by encapsulating Kiton Red in the microdroplets of a water-oil-water emulsion, so-called double-bubbles. The existence of KR in free solution in the inner water phase of the droplet preserves the response of its fluorescence lifetime to temperature. There is a slight perturbation to the fluorescence decay of the encapsulated KR, as a result of aggregation at the relatively high concentration used, but the temperature dependence of the fluorescence lifetime remains essentially identical to that in bulk aqueous solution.

Microdroplets with diameters between 5 and 20 μm have been trapped and manipulated by optical tweezers within a microfluidic flow. FLIM imaging of optically trapped microdroplets held at selected positions across a temperature gradient within a microfluidic device has enabled the non-invasive measurement of local

temperature in a microchannel, with a temperature resolution of about 1 ^{o}C and micron-scale spatial resolution. Greater temperature resolution could easily be achieved by microdroplet-encapsulation of a more sensitive fluorescent probe, such as a thermo-responsive polymer[17].

In view of the ease of fabrication of the fluorescent microdroplets and the existence of a variety of sophisticated multi-beam optical tweezer modalities, we anticipate that the combined use of optical tweezers and FLIM has much to offer in the field of microfluidic temperature measurement. Moreover this approach could be readily extended to other measurands by the adoption of suitably functionalised fluorescent microspheres.

References

[1] C. S. Liao, G. B. Lee, J. J. Wu, C. C. Chang, T. M. Hsieh, F. C. Huang and C. H. Luo, *Biosens. Bioelectron.*, 2005, **20**, 1341-1348.

[2] H. C. Chang, S. N. Leaw, A. H. Huang, T. L. Wuk and T. C. Chang, *J. Clin. Microbiol.*, 2001, **39**, 3466-3471.

[3] J. Li and C. Kleinstreuer, *Microfluid. Nanofluid.*, 2009, **6**, 661-668.

[4] P. Chamarthy, S. V. Garimella and S. T. Wereley, *Int. J. Heat Mass Tran.*, 2010, **53**, 3275-3283.

[5] H. B. Mao, T. L. Yang and P. S. Cremer, *J. Am. Chem Soc.*, 2002, **124**, 4432-4435.

[6] U. Seger, M. Panayiotou, S. Schnydrig, M. Jordan and P. Renaud, *Electrophoresis*, 2005, **26**, 2239-2246.

[7] G. Y. Tang, D. G. Yan, C. Yang, H. Q. Gong, J. C. Chai and Y. C. Lam, *Electrophoresis*, 2006, **27**, 628-639.

[8] D. Ross, M. Gaitan and L. E. Locascio, *Anal. Chem.*, 2001, **73**, 4117-4123.

[9] D. Ross and L. E. Locascio, *Anal. Chem.*, 2002, **74**, 2556-2564.

[10] J. Sakakibara, K. Hishida and M. Maeda, *Exp. Fluids*, 1993, **16**, 82-96.

[11] R. Samy, T. Glawdel and C. L. Ren, *Anal. Chem.*, 2008, **80**, 369-375.

[12] K. Chung, J. K. Cho, E. S. Park, V. Breedveld and H. Lu, *Anal. Chem.*, 2009, **81**, 991-999.

[13] D. A. Mendels, E. M. Graham, S. W. Magennis, A. C. Jones and F. Mendels, *Microfluid. Nanofluid.*, 2008, **5**, 603-617.

[14] R. K. P. Benninger, Y. Koc, O. Hofmann, J. Requejo-Isidro, M. A. A. Neil, P. M. W. French and A. J. deMello, *Anal. Chem.*, 2006, **78**, 2272-2278.

[15] F. Gielen, F. Pereira, A. J. deMello and J. B. Edel, *Anal. Chem.* **82**, 7509-7514.

[16] T. Robinson, Y. Schaerli, R. Wootton, F. Hollfelder, C. Dunsby, G. Baldwin, M. Neil, P. French and A. Demello, *Lab Chip*, 2009, **9**, 3437-3441.

[17] E. M. Graham, K. Iwai, S. Uchiyama, A. P. de Silva, S. W. Magennis and A. C. Jones, *Lab Chip*, **10**, 1267-1273.

[18] H. M. Shapiro, *Practical Flow Cytometry, Third edition*, *Wiley 1995*.

[19] H. Mushfique, J. Leach, H. B. Yin, R. Di Leonardo, M. J. Padgett and J. M. Cooper, *Anal. Chem.*, 2008, **80**, 4237-4240.

[20] B. A. Nemet and M. Cronin-Golomb, *Opt. Lett.*, 2002, **27**, 1357-1359.

[21] G. Knoner, S. Parkin, N. R. Heckenberg and H. Rubinsztein-Dunlop, *Phys. Rev. E*, 2005, **72**.

[22] A. Terray, J. Oakey and D. W. M. Marr, *Science*, 2002, **296**, 1841-1844.

[23] K. Ladavac and D. G. Grier, *Opt. Express*, 2004, **12**, 1144-1149.

[24] J. Leach, H. Mushfique, R. di Leonardo, M. Padgett and J. Cooper, *Lab Chip*, 2006, **6**, 735-739.

[25] J. Enger, M. Goksor, K. Ramser, P. Hagberg and D. Hanstorp, *Lab Chip*, 2004, **4**, 196-200.

[26] G. P. McNerney, W. Hubner, B. K. Chen and T. Huser, *J. Biophotonics*, **3**, 216-223.

[27] M. Capitanio, D. Maggi, F. Vanzi and F. S. Pavone, *J. Optics A-Pure Appl. Optics*, 2007, **9**, S157-S163.

[28] K. Ramser, W. Wenseleers, S. Dewilde, S. Van Doorslaer, L. Moens and D. Hanstorp, *J. Biomed. Optics*, 2007, **12**.

[29] R. R. Gullapalli, T. Tabouillot, R. Mathura, J. H. Dangaria and P. J. Butler, *J. Biomed. Optics*, 2007, **12**.

[30] N. Klauke, P. Monaghan, G. Sinclair, M. Padgett and J. Cooper, *Lab Chip*, 2006, **6**, 788-793.

[31] M. J. Snare, F. E. Treloar, K. P. Ghiggino and P. J. Thistlethwaite, *J. Photochem.*, 1982, **18**, 335-346.

[32] R. M. Sanchez-Martin, M. Muzerelle, N. Chitkul, S. E. How, S. Mittoo and M. Bradley, *Chembiochem*, 2005, **6**, 1341-1345.

[33] O. J. Miller, K. Bernath, J. J. Agresti, G. Amitai, B. T. Kelly, E. Mastrobattista, V. Taly, S. Magdassi, D. S. Tawfik and A. D. Griffiths, *Nature Methods*, 2006, **3**, 561-570.

[34] G. M. Whitesides, *Abstracts of Papers of the American Chemical Society*, 1996, **212**, 31-INOR.

[35] G. D. Wright, J. Arlt, W. C. K. Poon and N. D. Read, *Fungal Genet. Biol.*, 2007, **44**, 1-13.

[36] H. C. Gerritsen, M. A. H. Asselbergs, A. V. Agronskaia and W. Van Sark, *J. Microsc.*, 2002, **206**, 218-224.

[37] F. Gao, Z. G. Su, P. Wang and G. H. Ma, *Langmuir*, 2009, **25**, 3832-3838.

[38] D. S. Tawfik and A. D. Griffiths, *Nature Biotech.*, 1998, **16**, 652-656.

[39] A. D. Griffiths and D. S. Tawfik, *Trends Biotechnol.*, 2006, **24**, 395-402.

[40] D. Koley and A. J. Bard, *Proc. Natl. Acad. Sci.,* 2010, **107**, 16783–16787).

[41] N. Boens, W. Qin, N. Basaric, J. Hofkens, M. Ameloot, J. Pouget, J. P. Lefevre, B. Valeur, E. Gratton, M. Vandeven, N. D. Silva, Y. Engelborghs, K. Willaert, A. Sillen, G. Rumbles, D. Phillips, A. Visser, A. van Hoek, J. R. Lakowicz, H. Malak, I. Gryczynski, A. G. Szabo, D. T. Krajcarski, N. Tamai and A. Miura, *Anal. Chem.*, 2007, **79**, 2137-2149.

[42] J. Ghasemi, A. Niazi and M. Kubista, *Spectrochim. Acta Part a-Mol. Biomol. Spectrosc.*, 2005, **62**, 649-656.

[43] R. A. Lampert, S. R. Meech, J. Metcalfe, D. Phillips and A. P. Schaap, *Chem. Phys. Lett.*, 1983, **94**, 137-140.

[44] Y. Liu, D. K. Cheng, G. J. Sonek, M. W. Berns, C. F. Chapman and B. J. Tromberg, *Biophys. J.*, 1995, **68**, 2137-2144.

[45] A. Schonle and S. W. Hell, *Opt. Lett.*, 1998, **23**, 325-327.

[46] E. J. G. Peterman, F. Gittes and C. F. Schmidt, *Biophys. J.*, 2003, **84**, 1308-1316.

[47] S. Ebert, K. Travis, B. Lincoln and J. Guck, *Opt. Express*, 2007, **15**, 15493-15499.

[48] D. S. Elson, I. Munro, J. Requejo-Isidro, J. McGinty, C. Dunsby, N. Galletly, G. W. Stamp, M. A. A. Neil, M. J. Lever, P. A. Kellett, A. Dymoke-Bradshaw, J. Hares and P. M. W. French, *New J. Phys.*, 2004, **6.**

[49] H. M. Hertz, L. Malmqvist, L. Rosengren and K. Ljungberg, *Ultramicroscopy*, 1995, **57**, 309-312.]